Zeolitic imidazolate framework-8 nanoparticle: a promising adsorbent for effective fluoride removal from aqueous solution

Parwathi Pillai[1] · Swapnil Dharaskar[1] · Surendra Sasikumar[1] · Mohammad Khalid[2]

Abstract

Fluoride removal from living entities is the foremost task as it is a non-biodegradable and harmful pollutant mostly found in groundwater. Nowadays, the application of nanoparticles as an adsorbent of fluoride is becoming an intense research due to its high surface area. In the present study, zeolitic imidazolate framework-8 (ZIF-8) nanoparticles adsorption behavior and its efficiency in fluoride removal from an aqueous phase were studied. Various structures, sizes and morphologies of nanoparticles were investigated by Fourier-transform infrared spectroscopy, X-ray powder diffraction, scanning electron microscope, transmission electron microscopy, Raman spectroscopy and zeta seizer. By varying process parameters such as contact time, adsorbent dosage, stirring rate, temperature, and pH, batch adsorption was carried out. The optimum conditions for fluoride removal by ZIF-8 nanoparticles were found as contact time 15 min, adsorbent dosage 0.06 g/L, agitation rate 400 rpm, temperature 20 °C, pH 8. Pseudo-second order in kinetic study showcases that the regression coefficient was found to be 0.99. The experimental data of Langmuir isotherm model of adsorption system reveal the adsorption capacity of 90 mg/g which has better adsorption capacity than other adsorbents. The isothermal multistage adsorption was also studied to understand the mechanism of adsorption of ZIF-8 nanoparticles for fluoride removal. The result in the present work gives a promising adsorbent for the fluoride removal.

Keywords Adsorption · Fluoride · Nanoparticles · Zeolitic imidazolate framework-8

Introduction

Fluoride ions are found in animals, plants, food, soil and air. In more than 35 nations around the globe, people have found fluoride in excess in drinking water. The concentration and sternness depend upon the environmental situations which include geological and economic prominence (Teutli-Sequeira et al. 2014). The fluoride which is helpful in the living body for strengthening bones and cavities is in the range of 1.0 mg/L. According to the report of the World health organization (WHO), the maximum tolerance limit of fluoride in the drinking water is 1.5 mg/L. In human beings, the harmful cause due to fluoride is in dental and skeletal fluorosis. Dental fluorosis mainly affects the teeth, where it causes enamel and cavities problem. It also decreases the mineral content of teeth. The abnormal development of teeth can occur when the fluoride consumption is higher than the tolerance limit value (Çengeloğlu et al. 2002). Fluoride affects not only the human beings but also the plant species. India is not the only nation which has been affected by fluorosis; the problem has spread worldwide in developing countries such as Argentina, Australia, Algeria, USA, Libya, Turkey, Iran, China, Iraq, Sri Lanka, Canada, Thailand, Japan, South Africa, Kenya and New Zealand. The greatest effects of minerals, on the hydrogeochemistry of fluoride, are fluorite, apatite, mica, amphiboles, certain clays and villiamite. Almost all water of groundwater was found to be vary from the 5–50 mg/L concentrations. The health problems in the human body, plants and cattle occur due to the fluoride present in water as the fluoride contamination is more extensive in India (Kusrini et al. 2015).

✉ Swapnil Dharaskar
Swapnil.dharaskar@sot.pdpu.ac.in;
swapnildharaskar11@gmail.com

[1] Department of Chemical Engineering, School of Technology, Pandit Deendayal Petroleum University, Raisan, Gandhinagar, Gujarat 382007, India

[2] Graphene and Advanced 2D Materials Research Group (GAMRG), School of Science and Technology, Sunway University, Subang Jaya, Selangor, Malaysia

The methods for defluoridation include ion exchange, precipitation, activated alumina, electrocoagulation, reverse osmosis, precipitation and adsorption process. From all these methods, most of them are not favorable to use due to their high operational and maintenance costs, toxic by-products and their complex treatment. In the membrane process, problems such as high cost and fouling, scaling and degradation have more chances. The electrochemical method is not widely used due to its cost during maintenance and installation. The new method has been introduced by NEERI, the Nalgonda technique for defluoridation. This technique is used in developing countries where water purification problem occurs such as India, Kenya, Tanzania and Senegal. In this technique, the desired amount of alum, lime and bleaching powder is mixed with water and treated with flocculation, sedimentation, filtration and disinfection. This process takes 2 to 3 h for approximately 200 people in batches. The drawback of this method is the formation of a high amount of sludge and high residual aluminum concentration. Among the above methods, the adsorption is the most widely used technique due to its less cost, no maintenance, and availability of a broader range of adsorbent (Tomar and Kumar 2013).
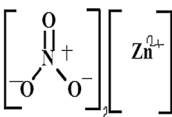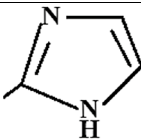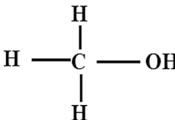
Nowadays in different research groups, the efficient adsorbent is of great concern and the center of attention, so the advanced adsorbent may lead to rapid removal and fast adsorption of toxic impurities within few minutes in different applications. The particle size of material in the range of 1–100 nm was defined as nanoparticles. They have novel size- and shape-dependent properties which can help the adsorbent for faster adsorption. Nanomaterial has been extensively used for over a decade and is effectively used in a wide range of applications. Recently, the nano-science and nanotechnology have shown a tremendous potential in the environmental problem such as water and wastewater. A diversity of efficient, economical and eco-friendly nanomaterials with unique functions was developed in different applications such as removal of toxic agents from industrial effluents, groundwater, drinking water and surface water (Gupta et al. 2015).

In this context, zeolitic imidazolate framework-8 (ZIF-8) chemical formula Zn(2-methylimidazole) has been considered to be an effective adsorbent for fluoride removal. ZIF-8 has sodalite-related zeolite-type structure comprising narrow six-membered ring pore windows which is 3.4 Å and much larger pores structure with thermal and chemical stabilities. ZIF-8 nanoparticles (ZIF-8 NPs) have been used as a novel adsorbent to achieve high adsorption capacity and greater active sites (Jiang et al. 2013). Here, fluoride ions get filled in the void space of ZIF-8 NPs, and thus the adsorption phenomenon occurs. This process directly increases the efficiency of removal of fluoride from water.

In the present work, ZIF-8 NPs were prepared and their structural, physical and chemical properties were characterized by using FTIR, XRD, SEM, TEM, Raman and zeta seizer. The batch adsorption was carried out by synthesized ZIF-8 NPs. Optimization of parameters such as adsorbent dosage, temperature, stirring rate, pH and contact time was carried out. Thermodynamic behavior, kinetic study and isotherm were also investigated. In the isotherm model to examine the equilibrium behavior of the system, the Langmuir and Freundlich isotherms were used. For better economy, the regeneration technique was also examined to novel

Table 1 Chemicals used for the synthesis of nanoparticles

Name	Formula	Structure	Density g/cm^3	Purity %	Make
Zinc nitrate	$Zn(NO_3)_2.6H_2O$		2.065	99	Sigma Aldrich
2-methylimidazole (Hmim)	$C_4H_6N_2$		-	99.8	Sigma Aldrich
Methanol	CH_3OH		792	99	Sigma Aldrich

adsorbent. To our best knowledge, the literature on the fluoride adsorption using ZIF-8 NPs as an adsorbent for fluoride removal is not available.

Experimental work

Chemicals and methods

The details of the chemicals used in the present work are shown in Table 1. All the chemicals are used without treatment and purification.

ZIF-8 nanoparticles synthesis

ZIF-8 NPs were synthesized using Zn $(NO_3)_2$.6H$_2$O (2.933 g) in methanol (200 mL) and quickly transferred to a in beaker containing Hmim (6.489 g) with methanol (200 mL) under vigorous stirring. Then, the mixture was kept for 1 h to react. The mixture slowly turned turbid with white milky color. Afterwards, the mixture was kept in a rotary evaporator for methanol recovery. Then, the remaining solution was centrifuged at 2000 rpm for 10 min and simultaneously washed with fresh methanol thrice. The NPs were dried in a vacuum oven at 79 ºC for 30 min. The schematic diagram of the entire process is shown in Fig 1.

Instrumentation

This instruments which were used for the present work and also for the characterization of particles include a Thermo Scientific Orion Fluoride electrodes which were used to analyze fluoride in the aqueous phase; a digital pH meter (Spectral Lab Instrumental Pvt. Ltd., India) was used to measure pH. From Fourier-transform infrared spectroscopy (FTIR) spectrometer the functional group were observed in ZIF-8NPs. X-ray powder diffraction (XRD) analysis was performed by X-ray diffractometer (PAN analytical X'pert PRO) by Cu X-ray tube ($\lambda = 1.5406$ Å) to know the phases present in the powdered sample. The structure, size and morphology of the ZIF-8 were investigated by field emission scanning electron microscopy (SEM) using (Zeiss LSM 510 Meta). Elemental analysis was done by energy-dispersive spectroscopy (EDS) attached to SEM. The sample was coated with gold for conductivity. To know the particle detail morphology, transmission electron microscopy (TEM) was conducted on Tenai 200 microscopic. Raman analysis was done on Renshaw spectroscopy at 2 cm^{-1}. To know the size of nanoparticles, zeta seizer (Malvern Panalytical Nano ZS90) was used.

Batch adsorption studies

To know the fluoride removal, the adsorption batch study was performed with the adsorbent with different factors. In each experimental run, 10 mg/L concentration of aqueous fluoride solution of 10 mL quantity and the known amount of ZIF-8 NPs were taken in a 100-mL flask. The flasks were agitated at a constant shaking rate at different factors which affected the fluoride removal in a controlled orbital shaker (G-30 MiuLab, China). After shaking, the samples were collected in a centrifuge (REMI R-23). The study of fluoride determination was performed by the fluoride ion-selective electrode (Thermo Scientific Orion Fluoride electrodes 720 A$^+$ ion analyzer, USA). The amount of fluoride is given by Eq. (1) as follows:

$$\%E = \frac{C_e - C_0}{C_e} \times 100 \tag{1}$$

where C_0 is the initial concentration of fluoride (g/L) and C_e is the equilibrium concentration of fluoride with nanoparticles (g/L).

Adsorption behavior

Adsorption kinetics

Pseudo-first-order and pseudo-second-order models are the adsorption kinetics which was performed for ZIF-8 NPs. Lagergren equation was also recognized as the pseudo-first-order kinetics. The equations are given as follows (Patnik et al. 2016)

$$\frac{dq_e}{dt} = k_1 \left(q_e - q_t \right) \tag{2}$$

where q_e and q_t are represented as the amount of fluoride adsorbed by adsorbent (mg/g) at equilibrium and at contact time t (min). After integrating Eq. 2 and rearranging at conditions at $t = 0$, $q_t = 0$ and $t = t$, $q_t = q_t$, it becomes

$$\ln \left(q_e - q_t \right) = \ln q_e - k_1 t \tag{3}$$

The pseudo-second order developed by Ho and McKay is represented by Eq. 4 (Ho and McKay 1998)

$$\frac{dq_t}{dt} = k_2 \left(q_e - q_t \right)^2 \tag{4}$$

where k_2 is the equilibrium constant (g/mg/min). After integrating Eq. 4 and rearranging the conditions, the equation is modified as given in Eq. 5

$$\frac{t}{q_t} = \frac{1}{k_2 q_e^2} + \frac{t}{q_e} \tag{5}$$

Adsorption isotherm

The adsorption isotherm was studied to know the adsorption properties and equilibrium parameters, and it also indicates the interaction among the molecules of adsorbate and adsorbent. It was fitted on Langmuir and Freundlich isotherms to know fluoride ions on ZIF-8 adsorbent. The equation is expressed as follows (Madan et al. 2016).

$$\frac{1}{Q_e} = \frac{1}{q_m b C_e} + \frac{1}{q_m} \tag{6}$$

where q_m is the maximum fluoride adsorption capacity (mg/g), Q_e and C_e are the equilibrium adsorption capacity (mg/g), b is the constant and the concentration of fluoride at equilibrium in the solution (mg/L).

The Freundlich isotherm shows the equation that applies the adsorption on heterogeneous surface interaction with the adsorbed species and also it is not applied to monolayer (Li et al. 2001). This isotherm indicates that the concentration of adsorbent surface increases with the decrease in adsorption energy.

$$\log Q_e = \log K_f + \frac{1}{n} \log C_e \tag{7}$$

where K_f is the measure of adsorption capacity and $1/n$ is the adsorption intensity of the heterogeneous system (Dey et al. 2014).

Thermodynamic study

Chemical reaction achieves equilibrium at one state. The parameters which involve in thermodynamic study are the entropy change (ΔS), enthalpy change (ΔS) and Gibbs free energy (ΔG). The equations are as follows.

$$\Delta G = RT \ln K_C \tag{8}$$

$$\Delta G = \Delta H - T\Delta S \tag{9}$$

$$\log\left(\frac{q_e m}{C_e}\right) = \frac{\Delta S°}{2.303R} + \frac{-\Delta H°}{2.303RT} \tag{10}$$

where K_c is the equilibrium constant, R is the universal constant (8.314 J/mol/K) and T is the absolute temperature. The plot of K_c versus $1/T$ gives the slope and intercept which are considered as ΔH and ΔS (Wu et al. 2007).

Results and discussion

Characterization of materials

After the NPs synthesis, FTIR was evaluated to indicate the presence of the functional group in the adsorbent, which is shown in Fig. 2. The bond formation is in the range of 400–4000 cm^{-1}. Preliminary stretching of N–H bonding is seen in 3500–3200 cm^{-1} band with a broad peak, and the other two small peaks are present at 3135 cm^{-1} and 2928 cm^{-1} which can be accredited to C–H stretching vibrational modes of the imidazole ring and of the methyl group present in the linker, respectively. C=N stretch modes peak at 1590 cm^{-1}, whereas the entire ring stretching corresponds to intense peaks at 1382 cm^{-1}. Several spectral bands are seen in the range 1350 to 900 cm^{-1} that could be qualified to the in-plane bending of the ring, and the peaks at 750 and 690 cm^{-1} were associated with aromatic sp^2 C–H bending. In addition, it has been observed that many miscellaneously weak peaks existed between the peaks; this may be due to the development of protonated groups by water clusters (Hu et al. 2011).

Further to confirm the synthesis, X-ray diffraction pattern analysis was performed to discover the phase of ZIF-8 that is shown in Fig. 3. The diffraction pattern having a peak at 2Θ values of 12.6°, 15.0°, 17.9°, 17.9°, 22°, 24.4°, 27.8°,28.5°,29.6°, 32.6° corresponding to the characteristic peaks (112), (022), (013), (222), (114), (233), (134), (044), (244) and (235) indicates the high crystalline plane of ZIF-8 NPs, and it is in good agreement with the sodalite structure of ZIF-8 shown in Fig. 2 (Jian et al. 2014).

Simultaneously, the morphology of ZIF-8 nanoparticles was studied by SEM analysis and TEM analysis was used
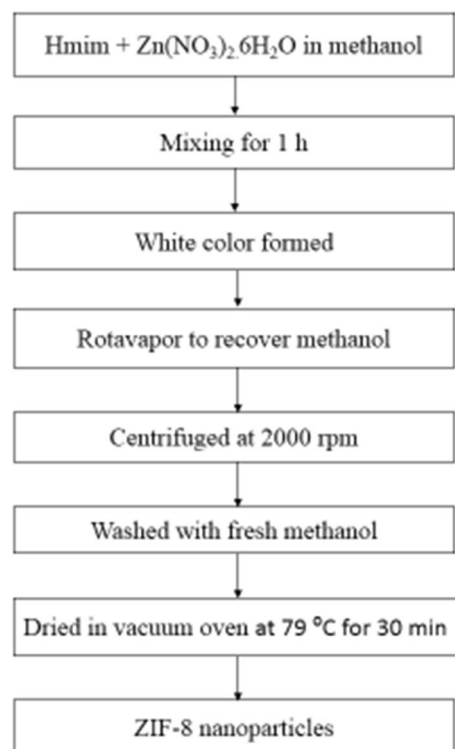

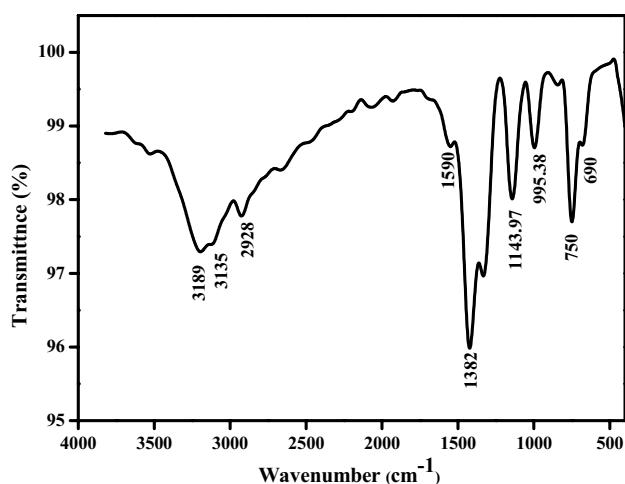**Fig. 1** Schematic diagram of preparation method for ZIF-8 nanoparticles

Fig. 2 FTIR spectra of ZIF-8 NPs

Fig. 3 XRD diffraction pattern of ZIF-8 NPs

to study the molecule structure, as shown in Fig. 4a, b, c. It has clearly indicated that nanoparticles were of hexagonal shape. This may be due to the faster growth kinetics forming during synthesis process. However, the morphology directly showcases the adsorption performance, specific surface area and the number of adsorptive sites of adsorbents (Jiang et al. 2016). The TEM image indicates the smooth surface which corresponds to SEM image. This further confirms the core shell structure microspheres shown in Fig. 4b, c (El-Hankari et al. 2016).

The Raman spectra were performed to know the structural fingerprint of molecules. The Raman spectra of ZIF-8 are shown in Fig. 5. The peak of Zn–N is observed at 282 cm^{-1}. The other high intensities were attributed at 678, 1142, 1161 and 1488 cm^{-1} of imidazolium ring, C–N stretching and C–H stretching, respectively. These bands are also assigned to the vibrational modes of the 2-methylimidazolate ligand (Tanaka et al. 2015). The zeta seizer shows particle size range of ZIF-8 nanoparticles from 200–300 nm as same as that shown by TEM in Fig. 6 (Kaur et al. 2017).
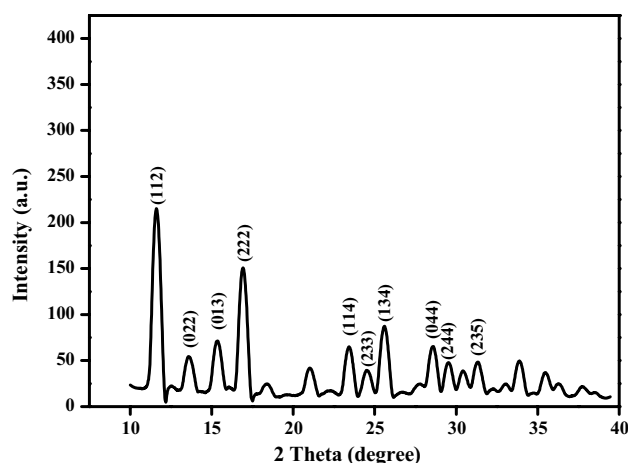
Effect of various parameters which affects fluoride removal adsorption

Subsequent to the effective ZIF-8 synthesis, the efficiency of this material was investigated to know the potential in fluoride by the adsorbent on factors which are affecting fluoride removal.

Influence of adsorbent dose

The study of batch experiment was conducted to examine the effects of adsorbent dose of ZIF-8 on the efficiency of fluoride removal, as shown in Fig. 7a. The fluoride removal increased in 0.01 to 0.06 g/L, but after 0.06 g/L no such increment was shown; further this dose remained constant till 1.0 g/L dose. The fluoride removal efficiency of ZIF-8 increased and then remained constant after a certain period of dose. The increment was shown in the range of 0.02 to 0.06 g/L dose, but it gradually became stable after the rise in dosage due to inaccessibility of active sites. The fluoride removal efficiency of 92% was achieved in 0.06 g/L dose of

Table 2 Comparison of adsorption capacity with other adsorbents

Adsorbent	Adsorbent dose (g/L)	Fluoride concentration (mg/L)	pH	Fluoride adsorbed (mg/g)	References
Chitosan iron complex	2	50	5–6	2.3	Hu et al. (2011)
Lanthanum-incorporated chitosan beads	0.4	20	5	4.7	Teutli-Sequeira et al. (2014)
Fe–Al–Ce trimetal hydroxide	–	19	6.5	4.46	Li et al. (2001)
Mg–Al–Fe hydrotalcite	0.2	10	6	14.0	Tomar and Kumar (2013)
Activated alumina	40	14	7	1.45	Wu et al. (2007)
Mesoporous alumina	4	5	3–9	8.26	Lee et al. (2010)
ZIF-8	0.06	10	8	90.90	Present study

مدينة الملك عبدالعزيز
KACST للعلوم والتقنية ⌃ Springer

Table 3 Kinetic constants and correlation coefficient

Initial fluoride concentration (mg/L)	Pseudo-first-order kinetic				Pseudo-second-order kinetic		
	$q_{e,expt}$ (mg/L)	$q_{e,cal}$ (mg/L)	K_1	R^2	$q_{e,cal}$ (mg/L)	K_2	R^2
10	2.7	1.09	0.367	0.89	2.94	1.12	0.99

Table 4 Langmuir isotherm and Freundlich isotherm of ZIF-8 nanoparticles for the adsorption of fluoride

Initial fluoride concentration (mg/L)	Langmuir isotherm		Freundlich isotherm	
10	q_m	90.90	K_f	0.764
	b	0.016	N	1.105
	R^2	0.925	R^2	0.72

ZIF-8. The same trend line was described by (Ekka et al. 2017).

Effect of contact time

Contact times in batch experiment were investigated for fluoride removal by keeping the dose 0.06 g/L with pH 8 followed by temperature 20 °C and stirring rate 400 rpm, as shown in Fig. 7b. In this adsorption process, the fluoride acceptance was found to increase till 5 min with the efficiency of 92%. After 5 min, the adsorption process slows down because of the inaccessibility of vacant sites which help in the fluoride adsorption. The contact time trend line is reported by (Jian et al. 2014).

Significance of temperature and agitation speed on adsorbent

The batch experiment was performed to examine the temperature and the stirring rate to know the effect of fluoride removal in the adsorbent, as shown in Fig. 7c and d. The temperature ranging from 5–35 °C was performed with 0.06 g/L of pH 8 till 5 min. It was detected that in initial temperature, the efficiency increases and at higher temperature the efficiency starts to decrease. According to Le Chatelier's principle, the fluoride efficiency decrease due to activation energy cause in reversible reaction which are more readily at lower temperature. Thus, adsorption increases at lower temperatures. The phenomenon of temperature was reported by (Smitha and Thampi, 2017).

The agitation rates were performed in the range of 0–500 rpm for both the adsorbents with 0.06 g/L of pH 7 till 5 min. Figure 7d shows that with the increase in the agitation speed, the fluoride removal efficiency increases. This is because as the agitation speed increases, the adsorbent and magnetic beads come in contact with each other, resulting in breaking of the adsorbent. Thus, breaking of adsorbent will increase the surface area and helps in fluoride removal in higher agitation speeds. The 400 rpm shows the optimum agitation speed for fluoride removal with maximum removal efficiency. After 400 rpm, the trend line remains constant due to the unavailability of active sites and no further break of adsorbent can be possible.

Influence of pH

The attraction between fluoride ion and the ZIF–8 depends on the pH. The investigation of pH was done in the range 2–12 to know the mechanism between them, as shown in Fig. 8. The result shows that the adsorption capacity increases with pH and then at a certain point decreases eventually as pH increases. In acidic medium, the fluoride ions are protonated partially forming the hydrofluoric acid, the pH in acidic medium adsorption is not as much as that in the neutral pH, while in the alkalinity the negative ions of fluoride and hydroxide ions repel, and therefore, it leads to a decrease in the adsorption capacity. The optimum pH obtained is 8 for fluoride removal using ZIF-8 as adsorbent. The similar pH trend line was also described by (Mohapatra et al. 2012).

Comparison literature study

Comparative literature study of fluoride adsorption on ZIF-8 and other adsorbents is given in Table 2. From this result, the efficiency of ZIF-8 is better than several other adsorbents studied in the literature in terms of different parameters such as dosage of adsorbent, time and adsorption capacity of fluoride. The possible reasons for the better fluoride removal

Table 5 Gibbs free energy data

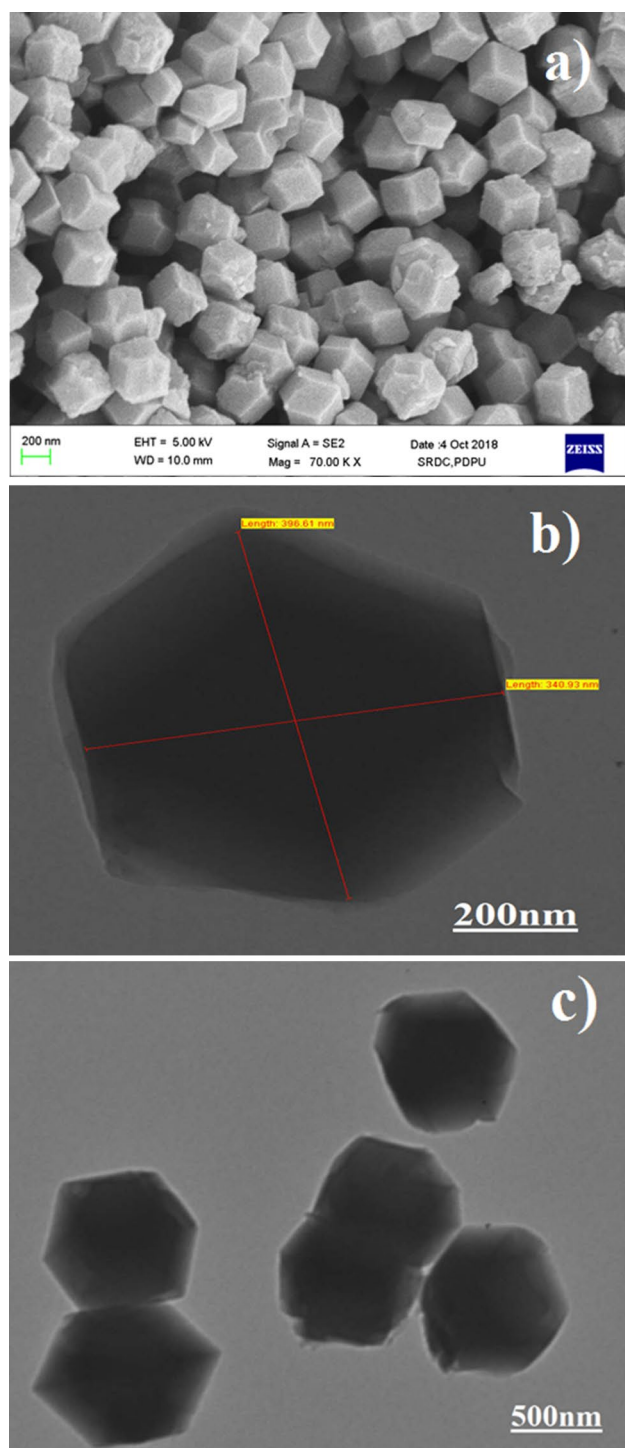| Initial fluoride concentration (mg/L)	$\Delta H°$ (kJ/mol)	$\Delta S°$ (kJ/K/mol)	$\Delta G°$ (kJ/mol)			
			15 °C	25 °C	30 °C	35 °C
10	−3.26	0.44	−3.34	−7.74	−9.94	−12.14

⚏ Springer

Fig. 4 **a** SEM image for 2 μm size **b**, **c** TEM image for 200 nm and 500 nm of ZIF-8 NPs
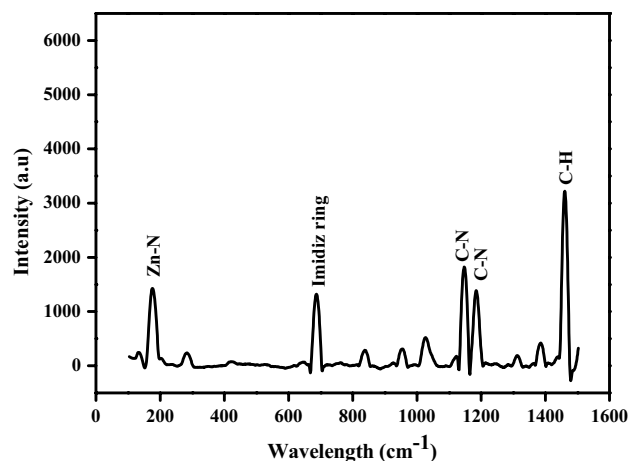

Fig. 5 Raman spectra of ZIF-8 NPs

using ZIF-8 nanoparticles are: (1) high surface area and (2) ion pair attraction between the ZIF-8 NPs and fluoride ions.

Adsorption kinetics

The adsorption kinetics study reveals about the mechanism of the adsorption with respect to equilibrium time. To investigate adsorption kinetics for the fluoride removal using ZIF-8 adsorbent, time reliant on pseudo-first order and pseudo-second order was applied, as shown in Fig. 9a, b and Table 3. Between these two models, the decisions were based on the regression coefficient (R^2) and the agreement made on experimental and calculated value of q_e.

The pseudo-first-order model assumes that the difference in the amount of solute and equilibrium concentration is directly proportional to the change in rate w.r.t time. The graph of ln ($q_e - q_t$) versus 't' plot provides the slope as rate constant k_1 and intercept as equilibrium adsorbate adsorbed q_e. The regression coefficient was found to be 0.89 for ZIF-8, as shown in Fig. 9b. This indicates that the first order was not suitable for the ZIF-8 as it does not agree with the experimental data ($q_{e,exp}$) and the calculated data ($q_{e,cal}$). It was stated from the result that pseudo-first order does not follow; thus, it is not a diffusion-controlled phenomena.

The pseudo-second-order model graph is plotted of t/q_e versus 't' giving the slope k_2 and q_e as corresponding regression coefficient (R^2) as 0.99, as shown in table and in Fig. 9. It was found that the qe values are well matched

with the experimental values, so this follows the pseudo-second order. That also states that it depends on the fluoride which is present in the aqueous phase and the active sites on the adsorbent of ZIF-8. The result of pseudo-first order and pseudo-second order is stated in Table 3 (Chai et al. 2013).

Adsorption isotherm studies

To investigate the adsorbent efficiency, the adsorption isotherm is used. It gives the information about the reaction feasibility and information such as adsorbent surface phenomenon. In this current work, experimental-related data were fitted in the isotherms such as Langmuir and Freundlich by varying initial concentrations (10–100 mg/L) with 0.06 adsorbent dose of the ZIF-8. The adsorption isotherm and adsorption parameters attained by the two models are displayed in Table 4 and Fig. 10. To obtain the design of the adsorption system, it was necessary to know the equilibrium curve suitable correlation. Assumption for the Langmuir isotherm is the evenly distributed adsorbent active sites on the surface, whereas active sites are same and only one molecule is attached to the adsorption on the surface; this mechanism is termed as monolayer adsorption. Further, there is no adsorbed molecules interrelation among them. The plot was $1/q_e$ and $1/C_e$, gives q_m and b and reveals a good prospective of the regression coefficient as 0.925 for synthesized adsorbent for the fluoride with the highest adsorption capacity of 90.90 mg/g, while in the Freundlich isotherm, the model gives a value of K_f and $1/n$ in the plot of log Q_e and log C_e in consort with 0.72 as regression coefficient reveals the fluoride absorption on ZIF-8 NPs (Biswas et al. 2010).

Thermodynamics study

The thermodynamics factors regulate the adsorption nature and possibility of the process. There are various thermodynamic factors such as enthalpy change (ΔH), free energy change (ΔG) and entropy change (ΔS) which were investigated in different ranges of temperature. The fluoride adsorption was best at moderate temperature, while it decreased when the temperature increased; this showcases that the fluoride–NPs interaction bond goes weaker at higher temperatures. Anionic–π and cationic–π, and the electrostatic interaction between fluoride ions and ZIF-8 are responsible for the firmness of these systems.

Henceforth, in the current study higher temperature for fluoride adsorption is not suitable, while lower temperatures are more favorable, connected to ΔG values attained at different temperatures. Gibbs free energy was calculated and is shown in Table 5. The reaction feasibility and spontaneous nature are indicated by negative ΔG values of the adsorption at a given temperature. In fluoride adsorption, ΔG value decreases with temperature rise and shows a degree of feasibility in an increased trend. Randomness increases at solid solution suggesting ΔS positive at the solid–solution interface. Moreover, increase in randomness indicates the increase in degrees of freedom at the ZIF-8 and fluoride solution interfaces, as shown in Fig. 11 (Dey et al. 2014).

Probable mechanism of fluoride adsorption

The mechanism of fluoride ion and the ZIF-8 NPs is shown in Fig. 12. The forces between Zn^{2+} and fluoride ion can form together electrostatic attraction. Moreover, the imidazolate involves the ion pair attraction with the F^- ion that will attract the adsorption. This makes the adsorption faster with the electrostatic properties of ZIF-8 with fluoride ion. And the fluoride ion has high electron affinity; it helps Zn^{2+} and $hmim^+$ attract each other.

Regeneration study

The effect of the regeneration of ZIF-8 was demonstrated using batch experiments. The stages were carried out at the optimal conditions to know the adsorption of fluoride in the regeneration cycle. The 10-ppm concentration was taken, and then the adsorbent was vigorously stirred in NaOH for 30 min. Further, it was centrifuged and dried at 90 °C. The adsorbent was maintained in the same optimal conditions for the rest of the stages. The result indicates that until the third stage, the fluoride removal efficiency achieved 87%. The efficiency decreased in the further fourth cycle because of the porous structure, where fluoride was adsorbed onto the surface and it may be possible that some fluoride may not have been removed completely. It gives a clear idea of reusability of NPs with respect to the number of cycles for fluoride removal which is shown in Fig. 13 (Sylvester et al. 2007).
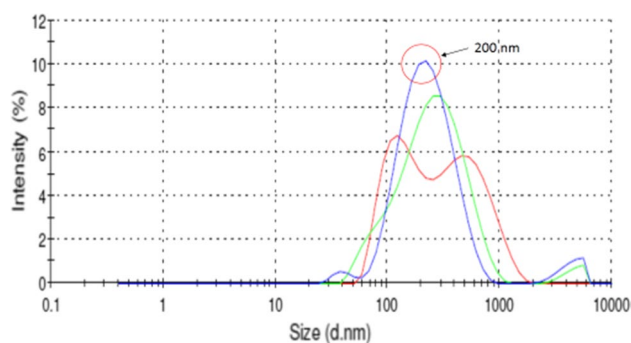
Fig. 6 Zeta seizer of ZIF-8 NPs

Conclusion

In the present work, ZIF-8 NPs were synthesized at room temperature in a single pot. The structure, size, crystallography and morphology were confirmed by FTIR, XRD, SEM, TEM, Raman and zeta seizer. More than 90% fluoride was adsorbed within 5 min adsorption time, temperature = 15 °C, adsorbent dosage = 0.06 g, pH = 8 and stirring rate = 400 RPM for 10 mg/L concentration of fluoride. The adsorption percentage was decreased gradually with increase in the initial fluoride concentration. Equilibrium data results showed that the fluoride adsorption on ZIF-8 nanoparticles follows Langmuir isotherm with an adsorption capacity of 90.9 mg/g which specifies monolayer adsorption on the nanoparticle surface. Estimation of thermodynamic adsorption
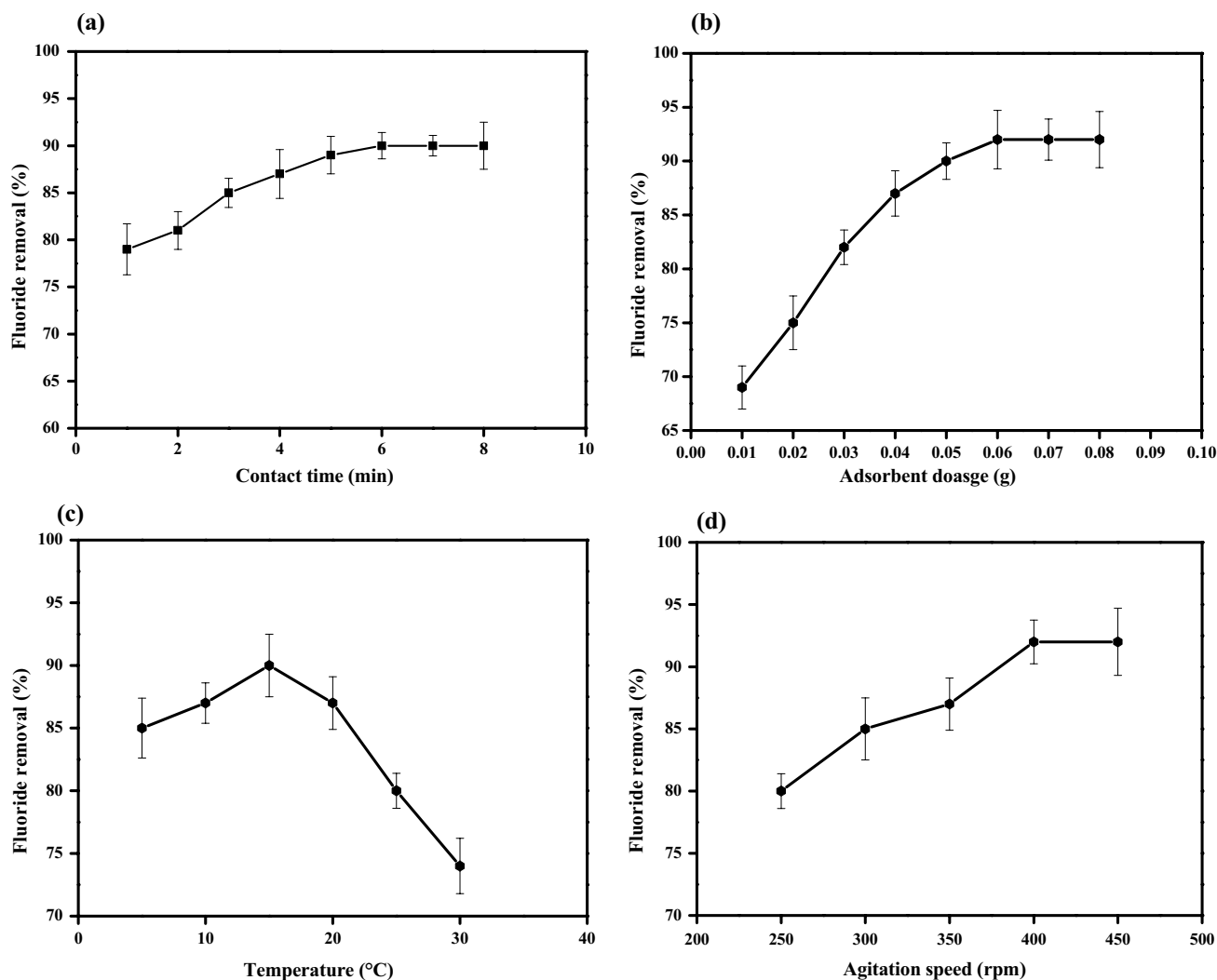
Fig. 7 Effect of **a** contact time, **b** adsorbent dose, **c** temperature and **d** agitation speed on fluoride removal
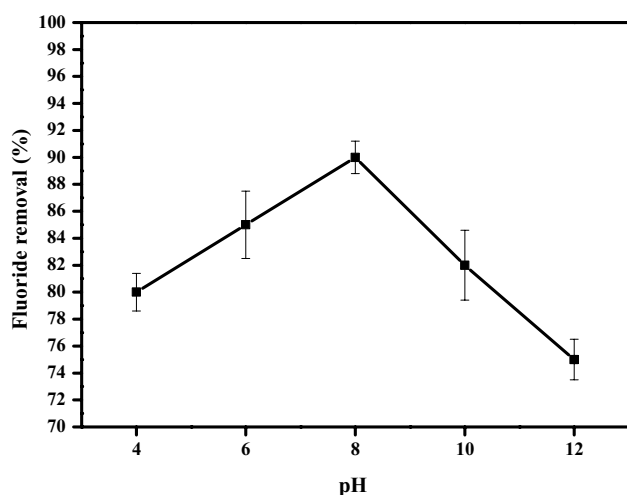
Fig. 8 Effect of pH on adsorption of fluoride
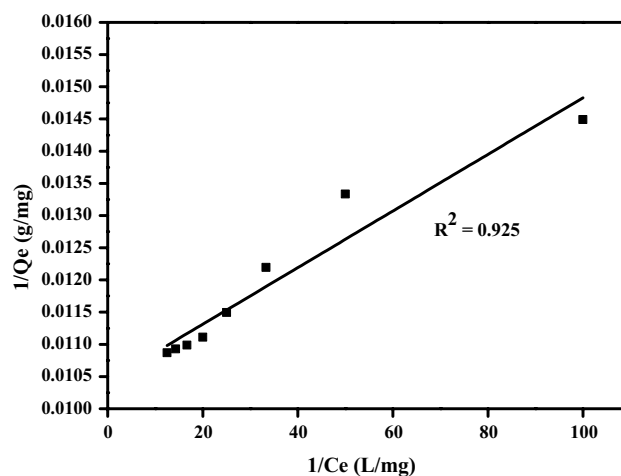
Fig. 10 Langmuir isotherm of fluoride adsorption in ZIF-8

study discloses that the $\Delta H°$ value -3.26 kJ/mol which was spontaneous and exothermic in nature further confirms the physicochemical adsorption process of fluoride. Regeneration study showed up to four cycles with NaOH solution and also indicated good adsorption efficiencies. Overall, this study demonstrated that the synthesized adsorbent may be considered as a promising adsorbent for the removal of fluoride from aqueous solution (Figs. 6, 7, 8, 9, 10, 11, 12, 13).
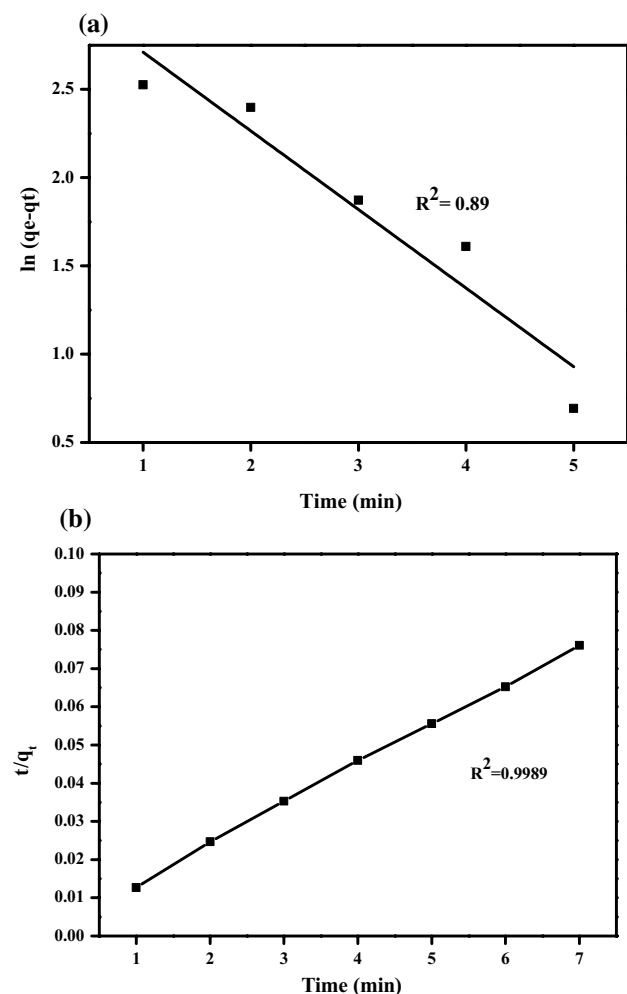
Fig. 9 a Pseudo-first-order kinetic plot; **b** pseudo-second-order kinetic plot
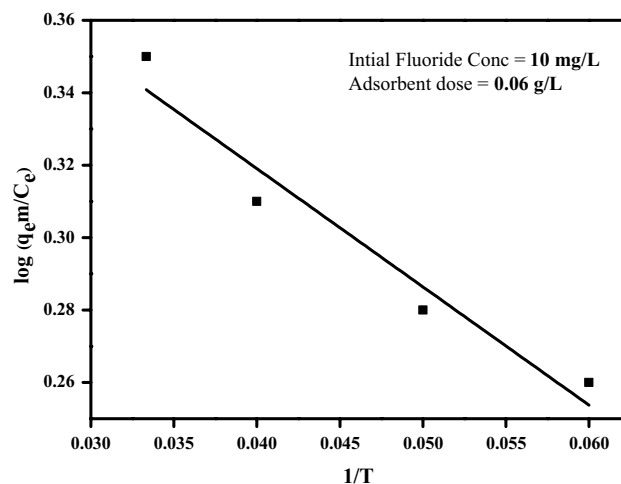
Fig. 11 Thermodynamic study of fluoride adsorption in ZIF-8
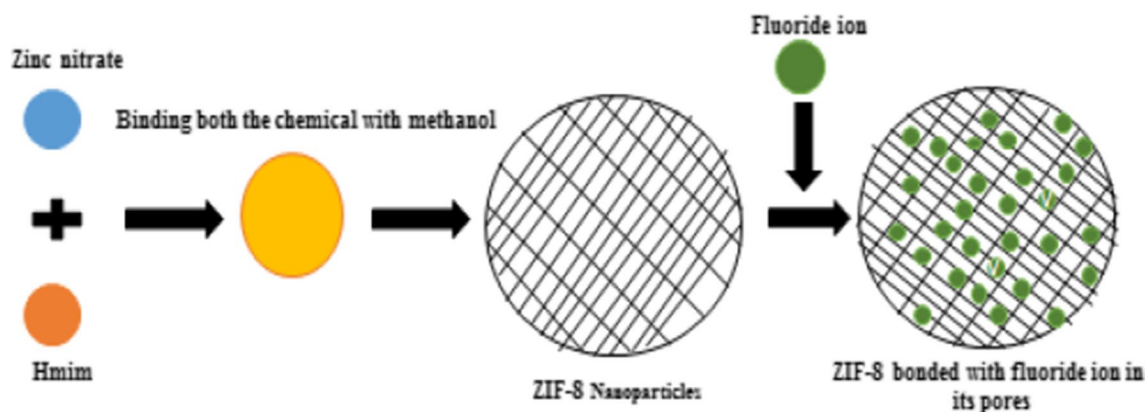
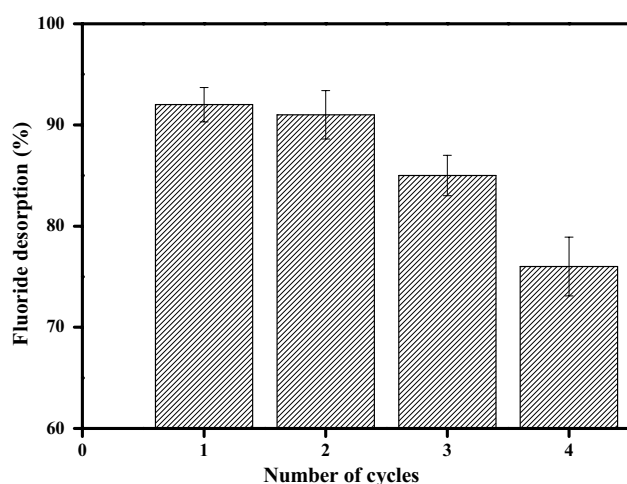**Fig. 12** Feasible defluoridation mechanism of ZIF-8

Fig. 13 Regeneration study for ZIF-8

Compliance with ethical standards

Conflict of interest The authors declare that they have no conflict of interest regarding the publication of this paper.

References

Biswas K, Gupta K, Goswami A, Ghosh UC (2010) Fluoride removal efficiency from aqueous solution by synthetic iron(III)-aluminum(III)-chromium(III) ternary mixed oxide. Desalination 255:44–51

Çengeloğlu Y, Kır E, Ersöz M (2002) Removal of fluoride from aqueous solution by using red mud. Sep Purif Technol 28:81–86

Chai L, Wang Y, Zhao N, Yang W, You X (2013) Sulfate-doped Fe_3O_4/Al_2O_3 nanoparticles as a novel adsorbent for fluoride removal from drinking water. Water Res 47:4040–4049

Dey A, Singh R, Purkait MK (2014) Cobalt ferrite nanoparticles aggregated schwertmannite: a novel adsorbent for the efficient removal of arsenic. J Water Process Eng 3:1–9

Ekka B, Dhaka RS, Patel RK, Dash P (2017) Fluoride removal in waters using ionic liquid-functionalized alumina as a novel adsorbent. J Clean Prod 151:303–318

El-Hankari S, Aguilera-Sigalat J, Bradshaw D (2016) Surfactant-assisted ZnO processing as a versatile route to ZIF composites and hollow architectures with enhanced dye adsorption. J Mater Chem A 4:13509–13518

Gupta VK, Tyagi I, Sadegh H, Ghoshekand RS, Makhlouf ASH, Maazinejad B (2015) Nanoparticles as adsorbent; a positive approach for removal of noxious metal ions: a review. Sci Technol Dev 34:195–214

Ho YS, McKay G (1998) The kinetics of sorption of basic dyes from aqueous solution by sphagnum moss peat. Can J Chem Eng 76:822–827

Hu Y, Kazemian H, Rohani S, Huang Y, Song Y (2011) In situ high pressure study of ZIF-8 by FTIR spectroscopy. Chem Commun 47:12694–12696

Jian M, Liu B, Zhang G, Liu R, Zhang X (2014) Adsorptive removal of arsenic from aqueous solution by zeolitic imidazolate framework-8 (ZIF-8) nanoparticles colloids and surfaces A: physicochemical and Engineering aspects adsorptive removal of arsenic from aqueous solution by zeolitic imidazolate. Colloids Surf A Physicochem Eng Asp 465:67–76

Jiang J, Yang C, Yan X (2013) Zeolitic imidazolate framework-8 for fast adsorption and removal of benzotriazoles from aqueous solution. ACS 5(19):9837–9842

Jiang M, Cao X, Liu P, Zhang T, Zhang J (2016) ZIF-8@polyvinylpyrrolidone nanocomposites based N-doped porous carbon for highly efficient oxygen reduction reaction in alkaline solution. J Electrochem Soc 163:459–464

Kaur H, Mohanta GC, Gupta V, Kukkar D, Tyagi S (2017) Synthesis and characterization of ZIF-8 nanoparticles for controlled release of 6-mercaptopurine drug. J Drug Deliv Sci Technol 41:106–112

Kusrini E, Sofyan N, Suwartha N, Yesya G, Priadi CR (2015) Chitosan-praseodymium complex for adsorption of fluoride ions from water. J Rare Earths 33:1104–1113

Lee G, Chen C, Yang ST, Ahn WS (2010) Enhanced adsorptive removal of fluoride using mesoporous alumina. Microporous Mesoporous Mater 127:152–156. https://doi.org/10.1016/j.micro meso.2009.07.007

Li YH, Wang S, Cao A, Zhao D, Zhang X, Xu C, Luan Z, Ruan D, Liang J, Wu D, Wei B (2001) Adsorption of fluoride from water by amorphous alumina supported on carbon nanotubes. Chem Phys Lett 350:412–416

Madan SS, Wasewar KL, Ravi Kumar C (2016) Adsorption kinetics, thermodynamics, and equilibrium of α-toluic acid onto calcium peroxide nanoparticles. Adv Powder Technol 27:2112–2120

Mohapatra M, Hariprasad D, Mohapatra L, Anand S, Mishra BK (2012) Mg-doped nano ferrihydrite—a new adsorbent for fluoride removal from aqueous solutions. Appl Surf Sci 258:4228–4236

Patnik S, Mishra PC, Nayak RN et al (2016) Removal of fluoride from aqueous solution using chitosan-iron complex. J Anal Bioanal Tech 7:326

Smitha K, Thampi SG (2017) Experimental investigations on fluoride removal from water using nanoalumina-carbon nanotubes blend. J Water Resour Prot 9:760–769

Sylvester P, Westerhoff P, Möller T, Badruzzaman M, Boyd O (2007) A hybrid sorbent utilizing nanoparticles of hydrous iron oxide for arsenic removal from drinking water. Environ Eng Sci 24:104–112

Tanaka S, Fujita K, Miyake Y, Miyamoto M, Hasegawa Y, Makino T, Van Der Perre S, Cousin Saint Remi J, Van Assche T, Baron GV, Denayer JFM (2015) Adsorption and diffusion phenomena in crystal size engineered ZIF-8 MOF. J Phys Chem C 119:28430–28439

Teutli-Sequeira A, Solache-Ríos M, Martínez-Miranda V, Linares-Hernández I (2014) Comparison of aluminum modified natural materials in the removal of fluoride ions. J Colloid Interface Sci 418:254–260

Tomar V, Kumar D (2013) A critical study on efficiency of different materials for fluoride removal from aqueous media. Chem Cent J 7:1

Wu X, Zhang Y, Dou X, Yang M (2007) Fluoride removal performance of a novel Fe–Al–Ce trimetal oxide adsorbent. Chemosphere 69:1758–1764